

Electromagnetic dipole moments of the top quark

Antonio O. Bouzas and F. Larios*

Departamento de Física Aplicada, CINVESTAV-Mérida,

A.P. 73, 97310 Mérida, Yucatán, México

Recent measurements like the $t\bar{t}\gamma$ production by CDF as well as the $\text{Br}(B \rightarrow X_s\gamma)$ and $A_{CP}(B \rightarrow X_s\gamma)$ are used to constrain the magnetic and electric dipole moments of the top quark. The $B \rightarrow X_s\gamma$ measurements by themselves define an allowed parameter region that sets up stringent constraints on both dipole moments. Actually, significantly more stringent than previously reported. The measurement by CDF has a $\sim 37\%$ error that is too large to set any competitive bounds, for which a much lower 5% error would be required at least. On the other hand, because of the LHC's higher energy (apart from its higher luminosity) the same measurement performed there could indeed further constrain the allowed parameter region given by the $B \rightarrow X_s\gamma$ measurement.

PACS numbers: 14.65.Ha, 12.15.-y

I. INTRODUCTION

The top quark stands out as the heaviest known elementary particle and its properties and interactions are among the most important measurements for present and future high energy colliders [1]. In particular, anomalous top dipole moments could point towards new physics (henceforth NP) effects like a composite nature of the top quark [2]. Concerning the anomalous magnetic and electric dipole moments (henceforth MDM and EDM, respectively) of the top quark, it is well known that the $\text{Br}(B \rightarrow X_s\gamma)$ can set up the most stringent constraints [3]. We will make a re-evaluation of those constraints, where in addition to the $\text{Br}(B \rightarrow X_s\gamma)$ we will consider a CP asymmetry for this process that indeed sets the strongest bounds on the EDM of the top quark. As we shall see, our bounds are more stringent than

* larios@mda.cinvestav.mx, corresponding author.

reported previously, and they are consistent with bounds that can be (indirectly) inferred from other studies. Recently, it has been suggested that another possible test of the MDM of the top quark could come from $H \rightarrow \gamma\gamma$ [4]. However, until such rare decay process gets more precise experimental analysis this option will not be feasible, and $b \rightarrow s\gamma$ along with $t\bar{t}\gamma$ production will remain the best probes of the MDM and EDM of the top quark. The CDF collaboration has reported a measurement of $t\bar{t}\gamma$ production with $6fb^{-1}$ of data [5]. (Some preliminary study has also been done for the LHC [6].) This process has been considered as a probe of the dipole moments of the top quark by Baur et. al [7] and their overall conclusion was that even though the Tevatron would not be able to set bounds as stringent as those from the $B \rightarrow X_s\gamma$ measurements, the LHC could. The reason for this is that since the dipole coupling is proportional to the momentum of the photon there is more relative contribution (compared to the QED coupling) as the energy of the collider increases. In this work, we take the experimental result by [5] and make an estimate of the bounds on the MDM and EDM, where indeed we corroborate that $t\bar{t}\gamma$ at the Tevatron is far from competing with $B \rightarrow X_s\gamma$. But on the other hand, we also find that the LHC could in principle set significant *direct* bounds that would further improve what we already have from the *indirect* bounds from $B \rightarrow X_s\gamma$.

II. THE MDM AND EDM OF THE TOP QUARK: PREVIOUS STUDIES.

Following [8], we define the effective $t\bar{t}\gamma$ Lagrangian

$$\mathcal{L}_{t\bar{t}\gamma} = e\bar{t} \left(Q_t \gamma_\mu A^\mu + \frac{1}{4m_t} \sigma_{\mu\nu} F^{\mu\nu} (\kappa + i\tilde{\kappa}\gamma_5) \right) t, \quad (1)$$

where the CP even κ and CP odd $\tilde{\kappa}$ terms are related to the anomalous MDM and EDM of the top quark, respectively. Similar Lagrangians are also defined in [3] and [7]. Comparing their different notations (notice a relative minus sign in the charge term) we obtain the following relations,

$$\begin{aligned} \kappa &= -F_{2V}^\gamma = \frac{2m_t}{e} \mu_t = Q_t a_t, \\ \tilde{\kappa} &= F_{2A}^\gamma = \frac{2m_t}{e} d_t, \end{aligned} \quad (2)$$

where $a_t = (g_t - 2)/2$ is the anomalous MDM in terms of the gyromagnetic factor g_t . The factors F_{2V}^γ and F_{2A}^γ are used in [7] and μ_t and d_t in [3]. The SM prediction for a_t is $a_t^{\text{SM}} = 0.02$

[9], which translates to $\kappa^{\text{SM}} = 0.013$. The bounds for κ that we will obtain will be about two orders of magnitude greater, therefore the SM prediction will not be considered in our calculations. On the other hand, the CP violating EDM factor d_t is strongly suppressed in the SM: $d_t^{\text{SM}} < 10^{-30} e \text{ cm}$ ($\tilde{\kappa} < 1.75 \times 10^{-14}$) [10]. The EDM is thus a very good probe of new physics. There are models with vector like multiplets that predict values as high as $10^{-19} e \text{ cm}$ ($\tilde{\kappa} < 1.75 \times 10^{-3}$) [11]. In fact, these models can also predict large values of other CP odd top quark properties like the chromoelectric dipole moment [12]. There are bounds based on the indirect effects on the EDM of the neutron, it has been found that $d_t < 3 \times 10^{-15}$ ($\tilde{\kappa} < 5.25 \times 10^1$) [13]. This is a rather weak bound compared to the ones we find below based on the branching ratio and the CP asymmetry of $b \rightarrow s\gamma$. As mentioned before, in [7] a study is made on the sensitivity of the Tevatron and the LHC to measure κ and $\tilde{\kappa}$ through $t\bar{t}\gamma$ production. Their conclusion for the Tevatron (with 8fb^{-1} of integrated luminosity) was that both coefficients could be probed in the range ± 5.2 at $68.3\%CL$. For the LHC at $\sqrt{s} = 14\text{TeV}$ the range would be about ± 0.2 assuming a 300fb^{-1} of data. As we shall see below those numbers are consistent with our conclusions, even though our strategy based on the $\sigma_{t\bar{t}\gamma}/\sigma_{t\bar{t}}$ ratio is different from the one used in [7].

The MDM and the EDM of the top quark have also been studied in the context of the $SU(2) \times U(1)$ gauge invariant effective Lagrangian [14]. For instance, a recent study on the ILC potential to probe the $t\bar{t}\gamma$ and $t\bar{t}Z$ vertices can be found in [15]. That study was made in the context of a minimal list of independent operators that give rise to couplings involving the top quark [16]. Indeed, the original list by Buchmuller and Wyler contains a long list of gauge invariant operators that were supposed to be independent [14]. It was found out some years later that some of the operators involving the top quark were in fact redundant [17]. A recent in-depth analysis made by Aguilar-Saavedra [16] has yielded a short list of only eight operators. More recently, a revised general list of all gauge invariant operators not necessarily related to the top quark was given in [18]. There are two, and only two, operators that give rise to both, the MDM and the EDM of the top quark [15],

$$\begin{aligned}\mathcal{O}_{uB\phi}^{33} &= C_{uB\phi}^{33} \bar{q}_{L3} \sigma^{\mu\nu} t_R \tilde{\phi} B_{\mu\nu} + h.c. , \\ \mathcal{O}_{uW}^{33} &= C_{uW}^{33} \bar{q}_{L3} \sigma^{\mu\nu} \tau^a t_R \tilde{\phi} W_{\mu\nu}^a + h.c.\end{aligned}\tag{3}$$

Comparing with the effective Lagrangian used in [15], we obtain the relations $d_V^\gamma = -\kappa/2$

and $d_A^\gamma = -\tilde{\kappa}/2$. Then, from Eq. (2.5) of [15]:

$$\begin{aligned}\kappa &= -\frac{2\sqrt{2}}{e} \frac{vm_t}{\Lambda^2} \text{Re}[s_w C_{uW}^{33} + c_w C_{uB\phi}^{33}] \\ \tilde{\kappa} &= -\frac{2\sqrt{2}}{e} \frac{vm_t}{\Lambda^2} \text{Im}[s_w C_{uW}^{33} + c_w C_{uB\phi}^{33}]\end{aligned}$$

Concerning the contribution from \mathcal{O}_{uW}^{33} the ATLAS collaboration has already set bounds on the real part of the coefficient [15, 19], $-1 < \Lambda^{-2} \text{Re}[C_{uW}^{33}] < 0.5 \text{TeV}^{-2}$. Moreover, we can also find a recent similar bound based on precision electroweak measurements [20], $-1.6 < \Lambda^{-2} \text{Re}[C_{uW}^{33}] < 0.8 \text{TeV}^{-2}$. This means that κ could only reach values of order 0.2 coming from this operator. We shall therefore ignore the effects from \mathcal{O}_{uW}^{33} and instead focus our attention on the operator $\mathcal{O}_{uB\phi}^{33}$. The contribution from this operator to the $b \rightarrow s\gamma$ process would indeed enter via the MDM and EDM terms of the $t\bar{t}\gamma$ vertex (in the unitary gauge) applied inside the loop associated to the C_7 Wilson coefficient [8]. From [20] we can find a recent bound on $C_{uB\phi}^{33}$, $-0.5 < \Lambda^{-2} \text{Re}[C_{uB\phi}^{33}] < 10.1 \text{TeV}^{-2}$. From the relation $\kappa = -0.34 \text{TeV}^2 \text{Re}[C_{uB\phi}^{33}] \Lambda^{-2}$ we conclude that the contribution from this operator should be in the range $-3.4 < \kappa < 0.17$. This range is similar to the limits we have found based on $b \rightarrow s\gamma$.

III. LIMITS FROM $t\bar{t}\gamma$ PRODUCTION AT THE TEVATRON

The CDF collaboration has reported a cross-section measurement of top-quark pair production with an additional photon that carries at least 10 GeV of transverse energy, $\sigma_{t\bar{t}\gamma} = 0.18 \pm 0.08$ pb [5]. In addition, using events with the same selection criteria as for the $t\bar{t}\gamma$ candidates, but without the photon, they also perform a measurement of the $t\bar{t}$ production cross section. In this way they determine the ratio $R^{\text{exp}} \equiv \sigma_{t\bar{t}\gamma}/\sigma_{t\bar{t}} = (0.024 \pm 0.009)$, in which systematic uncertainties are eliminated. That experimental result is in excellent agreement with the SM prediction $R^{\text{SM}} = 0.024 \pm 0.005$ [5].

The potential of using $t\bar{t}\gamma$ production at hadron colliders as a probe of the $t\bar{t}\gamma$ vertex was studied in [7] (following previous work in [21]). That production process can probe the charge of the top quark, including the presence of an axial-vector term, if any. The strategy proposed in [7] relies on analyzing the transverse-momentum distribution of the radiated photon, as the $\sigma_{\mu\nu}q^\nu$ dipole term tends to favor a greater p_T^γ . In this paper we assume that the dimension-4 $t\bar{t}\gamma$ coupling is as dictated by the Standard Model, so that possible NP

effects appear in the dipole terms only. Since the main result by CDF is given in terms of $\sigma_{t\bar{t}\gamma}/\sigma_{t\bar{t}}$, we consider that ratio as a function of the MDM κ and the EDM $\tilde{\kappa}$ to set bounds on those parameters. Although our strategy is simpler than the analysis carried out in [7], we believe it is yet useful to obtain an estimate of the sensitivity of the Tevatron result, and of future LHC results.

In order to quantify the impact of the top-quark MDM and EDM on the cross section, we focus our attention on the normalized ratio

$$\hat{R} \equiv \frac{R}{R^{\text{SM}}} = \frac{\sigma_{t\bar{t}\gamma}}{\sigma_{t\bar{t}\gamma}^{\text{SM}}}. \quad (4)$$

In this way, the CDF result can be translated to $\hat{R}^{\text{exp}} = 1 \pm 0.375$. We compute the cross sections for $p\bar{p} \rightarrow t\bar{t} \rightarrow bW^+\bar{b}W^-\gamma \rightarrow \text{FS}$ at leading order at the Tevatron energy, and the same processes with pp initial state at LHC energies. We choose semileptonic final states FS, as done in the CDF measurement, but consider also a simplified process with final state $bW^+\bar{b}W^-\gamma$ as a cross check of our results. For the numerical computation of the semileptonic cross section we consider the process $pp, p\bar{p} \rightarrow t\bar{t} \rightarrow b\bar{b}q q' \ell \nu_\ell \gamma$ with three lepton flavors, where the final photon can originate from any initial, intermediate or final charged particle. The calculation was carried out with MADGRAPH 5 [22], with the set of default parameters in which α , $\sin \theta_W$ and G_F are the primary parameters, but with $m_t = 173$ GeV. For the parton distributions functions we use the set CTEQ 6m for proton and antiproton with fixed renormalization and factorization scales set to m_t . Although not reported in detail here, we have explicitly checked that the dependence of our results on the choice of scale is quite weak.

In the radiative production process two modes are predominant: (1) $t\bar{t}$ produced along with the radiated photon followed by the decay of the top pair, which is indeed $t\bar{t}\gamma$ production proper, and (2) $t\bar{t}$ produced on-shell with one of them decaying radiatively (such as $t \rightarrow bW^+\gamma$). The first mode may involve initial-state radiation if the initial partons are charged. The second mode may involve final-state radiation from the b jets, the intermediate W boson or the W decay products. At the Tevatron energy $\sqrt{s} = 2$ TeV, the production of $t\bar{t}$ and $t\bar{t}\gamma$ receives its dominant contribution from $u\bar{u}$ initial states, but we take into account also the smaller contributions from initial $d\bar{d}$ and gg . The corresponding scattering amplitudes with two resonant top/antitop propagators involve a total of 876 Feynman diagrams, as given by MADGRAPH, of which 612 are independent. By analogy with the measurement reported by

CDF [5], we apply cuts in the transverse energy of the photon, missing transverse energy and pseudorapidity of the final particles given by

$$E_T^\gamma > 10\text{GeV}, \quad \cancel{E}_T > 20\text{GeV}, \quad |\eta_q| < 3.6, \quad |\eta_b| < 2, \quad |\eta_\gamma| < 1, \quad |\eta_\ell| < 1. \quad (5)$$

With those cuts we obtain a SM cross section $\sigma_{t\bar{t}\gamma}^{\text{SM}} = 0.07261$ pb at $\sqrt{s} = 2$ TeV, in agreement with the leading-order result reported in [5]. In order to increase the sensitivity of the process to the dipole moments of the intermediate top quarks it is necessary to reduce the background from photons originating in final-state charged particles. For that purpose we impose a lower bound on the distance from the photon to the charged particles in the η - ϕ plane, $\Delta = \sqrt{(\Delta\eta)^2 + (\Delta\phi)^2}$,

$$\Delta_{\gamma,\text{ch}} > 0.4, \quad (6)$$

which plays the same role as the analogous cuts introduced in the actual measurement [5]. With the cuts (5), (6) the SM cross section at 2 TeV is $\sigma_{t\bar{t}\gamma}^{\text{SM}} = 0.0193$ pb. We also perform the same computation for $t\bar{t}\gamma$ production in pp collisions at the LHC both at $\sqrt{s} = 7$ TeV and $\sqrt{s} = 14$ TeV. In this case the dominant contribution to the production process comes from gg initial states, but we also take into account the smaller contributions from the initial states $u\bar{u}$ and $d\bar{d}$. Thus, in particular, the set of Feynman diagrams involved in the scattering amplitudes is the same as in the previous case. With the cuts (5), (6), the SM cross sections at 7 and 14 TeV are $\sigma_{t\bar{t}\gamma}^{\text{SM}} = 0.1770$ and 0.8034 pb, respectively.

On the theoretical side, it is well known that at tree level the SM amplitude is real. The CP-even MDM κ term contributes linearly to the real part of the total amplitude, whereas the CP-odd EDM $\tilde{\kappa}$ contributes to its imaginary part only. Therefore, the expression for \hat{R} must have in general the quadratic form $\hat{R} = 1 + a_1\kappa + a_2\kappa^2 + b_2\tilde{\kappa}^2$. By computing \hat{R} for several values of κ and $\tilde{\kappa}$ we can obtain the coefficients a_i in \hat{R} at the desired energy. Then we use a relation of the form

$$\hat{R}_1 < \hat{R} = 1 + a_1\kappa + a_2\kappa^2 + a_3\tilde{\kappa}^2 < \hat{R}_2 \quad (7)$$

to find the allowed parameter region for $(\kappa, \tilde{\kappa})$ at that energy. In the case of the CDF measurement, we set $\hat{R}_{1,2} = 1 \pm 0.375$ to define the allowed region at the 1σ level. The computation of $\sigma_{t\bar{t}\gamma}$ for different values of κ , $\tilde{\kappa}$ was carried out by implementing the effective Lagrangian (1) in MADGRAPH by means of the program FEYNRULES 1.6.11 [23] (see also [24] for a more recent description). The resulting numerical coefficients in (7) are given by

$a_1 = -0.002, -0.008, -0.009$, $a_2 = 0.011, 0.055, 0.088$ and $a_3 = 0.011, 0.055, 0.089$ at the Tevatron and LHC energies: 2, 7 and 14 TeV, respectively.

IV. LIMITS FROM $B \rightarrow X_s \gamma$

In the context of effective lagrangians the $b \rightarrow s \gamma$ transition occurs through the effective Wilson coefficient $C_7(\mu)$, computed at the electroweak scale $\mu_h \gtrsim M_W$ from loop diagrams where the photon can be emitted either from the W boson or from the top quark [25]. NP effects on $C_7(\mu_h)$ can come from several different sources, for instance an anomalous $WW\gamma$ coupling. In this paper we are interested in the contributions from the MDM and EDM of the top quark to the effective $t\bar{t}\gamma$ vertex and, for simplicity, those are the only ones we will consider. Furthermore, the QCD running of $C_7(\mu)$ from the electroweak scale down to the bottom mass scale causes it to mix with other coefficients, so that $C_7(m_b)$ can receive NP contributions also from non-electroweak anomalous couplings. The main contribution of this type comes from the Wilson coefficient $C_8(\mu_h)$ associated with the $t\bar{t}g$ vertex. If we separate the SM value $C_7^{\text{SM}}(m_b) = -0.31$ from the NP contributions, the form of $C_7(m_b)$ in terms of the Wilson coefficients evaluated at μ_h is [25]

$$C_7(m_b) = -0.31 + 0.67 \delta C_7(\mu_h) + 0.09 \delta C_8(\mu_h) + \dots, \quad (8)$$

where $\delta C_i = C_i - C_i^{\text{SM}}$ and the ellipsis refers to terms containing other Wilson coefficients that make numerically smaller contributions. As mentioned above, we will focus only on the contributions to $C_7(m_b)$ arising from the MDM and EDM of the top quark. Thus, in (8) we set $\delta C_8(\mu_h) = 0$ and keep $\delta C_7(\mu_h)$ which is given by [8]

$$\begin{aligned} G_2 &= \frac{1}{4} - \frac{1}{x-1} + \frac{\ln x}{(x-1)^2} = 0.0908, \\ G_1 &= \frac{x/2 - 1}{(x-1)^3} (x^2/2 - 2x + 3/2 + \ln x) - G_2 = 0.0326, \\ C_7(\mu_h) &= C_7^{\text{SM}}(\mu_h) + \kappa G_1 + i\tilde{\kappa} G_2, \end{aligned} \quad (9)$$

with $x = (m_t/m_W)^2 = 4.63$. Notice that in (9) $C_7^{\text{SM}}(\mu_h) = -0.22$ is a real number, as is the CP-even MDM term proportional to κ , but the CP-odd EDM term in $\tilde{\kappa}$ adds an imaginary part to C_7 . This means that the $b \rightarrow s \gamma$ width, being proportional to $|C_7|^2$, will depend linearly and quadratically on κ , but only quadratically on $\tilde{\kappa}$. On the other hand, studies

that involve $b \rightarrow s$ transitions in general have been done that can set bounds on the real part of δC_7 : $-0.15 < \text{Re}(\delta C_7(\mu_h)) < 0.03$ [26]. Since from (9) we get $\text{Re}(\delta C_7(\mu_h)) = 0.0326\kappa$, the allowed region for κ would be $-5 < \kappa < 1$. This result is consistent with the bounds we obtain below based on the branching ratio for $B \rightarrow X_s \gamma$.

A. Limits from the branching ratio $\mathcal{B}(B \rightarrow X_s \gamma)$

An updated numerical expression for the branching ratio $\mathcal{B}(B \rightarrow X_s \gamma)$ in terms of the coefficients $C_7(\mu_h)$ and $C_8(\mu_h)$ can be found in eq. (4.3) of [27] which, retaining only LO contributions, can be written as

$$\begin{aligned} \delta \mathcal{B}(B \rightarrow X_s \gamma) &\equiv \mathcal{B}(B \rightarrow X_s \gamma) - \mathcal{B}^{\text{SM}}(B \rightarrow X_s \gamma) = 10^{-4} \times \\ &\times \left(\text{Re}(-7.184 \delta C_7 - 2.225 \delta C_8 + 2.454 \delta C_7 \delta C_8^*) + 4.743 |\delta C_7|^2 + 0.789 |\delta C_8|^2 \right), \end{aligned} \quad (10)$$

where $\delta C_{7,8}$ are defined as in (8) and it is understood that they are evaluated at the electroweak scale μ_h . The numerical coefficients in (10) were computed in [27] assuming a cut in the photon energy $E_\gamma > E_0 = 1.6$ GeV, as is conventionally done in this type of calculations and as will always be assumed in this paper in connection with the process $B \rightarrow X_s \gamma$. If the only NP effects we take into account are the MDM and EDM of the top quark, the coefficient $\delta C_7(\mu_h)$ appearing in (10) is given by (9), and $\delta C_8(\mu_h) = 0$.

In order to use (10) to constrain κ and $\tilde{\kappa}$ we need a predicted value for $\mathcal{B}^{\text{SM}}(B \rightarrow X_s \gamma)$ and a measured value for $\mathcal{B}(B \rightarrow X_s \gamma)$. For $\mathcal{B}^{\text{SM}}(B \rightarrow X_s \gamma)$ there are three recent calculations referred to in the literature, $10^4 \times \mathcal{B}^{\text{SM}}(B \rightarrow X_s \gamma) = (2.98 \pm 0.26)$ [28], (3.15 ± 0.23) [29], and (3.47 ± 0.48) [30]. A thorough discussion of those results can be found in [31]. For concreteness, we use in our calculations the value from [29]. The most recently updated experimental value is $\mathcal{B}^{\text{Exp.}}(B \rightarrow X_s \gamma) = (3.43 \pm 0.21 \pm 0.07) \times 10^{-4}$ [32] (see also the recent status report [33]). With those theoretical and experimental values, from (10) with δC_7 as given by (9), we get the relation

$$10^4 \times \delta \mathcal{B}(B \rightarrow X_s \gamma) = (3.43 \pm 0.22) - (3.15 \pm 0.23) = -0.234\kappa + 0.005\kappa^2 + 0.039\tilde{\kappa}^2. \quad (11)$$

which we use to set limits on $(\kappa, \tilde{\kappa})$.

B. Limits from the asymmetry $A_{\text{CP}}(B \rightarrow X_s \gamma)$

The CP asymmetry

$$A_{\text{CP}}(B \rightarrow X_s \gamma) = \frac{\Gamma(\bar{B} \rightarrow X_s \gamma) - \Gamma(B \rightarrow X_{\bar{s}} \gamma)}{\Gamma(\bar{B} \rightarrow X_s \gamma) + \Gamma(B \rightarrow X_{\bar{s}} \gamma)} \quad (12)$$

was first proposed in [34]. Its latest experimental value is quoted in [32] as $A_{\text{CP}}^{\text{Exp.}}(B \rightarrow X_s \gamma) = (-0.8 \pm 2.9)\%$. An expression for the asymmetry that includes the SM contribution as well as NP effects entering through the Wilson coefficients C_i with $i = 1, 7, 8$ is given in [35] (see also [36]). Since we are assuming $C_1 = C_1^{\text{SM}}$ and $C_8 = C_8^{\text{SM}}$ we can rewrite that expression in a simplified form. Following [35] we define the parameters r_7 , θ_7 as $r_7 e^{i\theta_7} = C_7(m_b)/C_7^{\text{SM}}(m_b)$. With $C_7(m_b)$ from (8) and $\delta C_7(\mu_h)$ from (9), they are found to be given by

$$r_7 e^{i\theta_7} = 1 - 0.0705\kappa - i0.1962\tilde{\kappa}. \quad (13)$$

We can then write eq. (13) of [35] as

$$A_{\text{CP}}[\%] = (a_7 + 0.5036d_7) \frac{\sin(\theta_7)}{r_7} + (0.6783 + 1.1550d_7) \frac{\cos(\theta_7)}{r_7} + \frac{0.0302}{r_7^2}, \quad (14)$$

$$a_7 = 16.6858 + 2.1400 \frac{\tilde{\Lambda}_{17}^c}{10\text{MeV}} + 3.9933 \frac{\tilde{\Lambda}_{78}}{100\text{MeV}}, \quad d_7 = \frac{\tilde{\Lambda}_{17}^u - \tilde{\Lambda}_{17}^c}{300\text{MeV}},$$

where the angle γ appearing in [35] has been set to $\gamma = 66.4^\circ$, as done in that reference. The dimensionless parameters a_7 , d_7 in (14) are linear combinations of the hadronic parameters $\tilde{\Lambda}_{17}^u$, $\tilde{\Lambda}_{17}^c$ and $\tilde{\Lambda}_{78}$, introduced in [35], that are related to the contribution of resolved photons to the asymmetry. The precise values of those hadronic parameters are not known, but their expected ranges of variation are estimated to be [35], $-330 < \tilde{\Lambda}_{17}^u < 525$ MeV, $-9 < \tilde{\Lambda}_{17}^c < 11$ MeV and $17 < \tilde{\Lambda}_{78} < 190$ MeV. Thus, for the parameters appearing in (14) we have $15.4387 < a_7 < 26.6271$ and $-1.1367 < d_7 < 1.7800$. This means, in particular, that the SM prediction $A_{\text{CP}}^{\text{SM}} = A_{\text{CP}}|_{\kappa=0=\tilde{\kappa}}$ is afflicted by a significant uncertainty, $-0.6\% < A_{\text{CP}}^{\text{SM}} < 2.8\%$.

We treat our ignorance of the hadronic parameters as a systematic uncertainty in the theoretical computation. Thus, we set

$$a_7 = \bar{a}_7 \pm \delta a_7 = 21.0329 \pm 5.5942, \quad d_7 = \bar{d}_7 \pm \delta d_7 = 0.3217 \pm 1.4583 \quad (15)$$

in (14), to obtain $A_{\text{CP}}(\kappa, \tilde{\kappa}) = \bar{A}_{\text{CP}}(\kappa, \tilde{\kappa}) \pm \delta A_{\text{CP}}(\kappa, \tilde{\kappa})$ with

$$\bar{A}_{\text{CP}}[\%] = A_{\text{CP}}[\%] \Big|_{\substack{a_7=\bar{a}_7 \\ d_7=\bar{d}_7}} = \frac{1.0801 - 0.0740\kappa - 4.1594\tilde{\kappa}}{(1 - 0.0705\kappa)^2 + 0.0385\tilde{\kappa}^2},$$

$$\begin{aligned}
\delta A_{\text{CP}}[\%] &= \frac{1}{r_7} \sqrt{\sin(\theta_7)^2 (\delta a_7)^2 + (1.1550 \cos(\theta_7) + 0.5036 \sin(\theta_7))^2 (\delta d_7)^2} \\
&= \frac{\sqrt{2.1267(1.1550 - 0.0814\kappa - 0.0988\tilde{\kappa})^2 + 1.2053\tilde{\kappa}^2}}{(1 - 0.0705\kappa)^2 + 0.0385\tilde{\kappa}^2}.
\end{aligned} \tag{16}$$

With the asymmetry written in this form, we can use its experimentally measured value to set bounds on the allowed region for $(\kappa, \tilde{\kappa})$.

V. ALLOWED PARAMETER SPACE FOR $(\kappa, \tilde{\kappa})$

We can now use (7), (11) and (16) to constrain the allowed region in the κ vs. $\tilde{\kappa}$ plane. For the branching ratio, the region allowed at the 1σ level is seen from (11) to be bounded by

$$-0.0383 < \delta\mathcal{B}(B \rightarrow X_s \gamma) < 0.5983. \tag{17}$$

That region is delimited in figures 1, 2 by gray solid lines. Roughly speaking the MDM is bounded to be $-2 < \kappa < 1$ which translated to the $m_t \mu_t = \kappa e/2 = 0.15\kappa$ term used in [3] means that $-0.3 < m_t \mu_t < 0.15$. Our limits are significantly more stringent than reported in [3].

With the experimental value for A_{CP} quoted above and its expression (16), at the 1σ level the asymmetry must satisfy the inequalities

$$-0.8 - \sqrt{2.9^2 + \delta A_{\text{CP}}[\%]^2} < \overline{A}_{\text{CP}}[\%] < -0.8 + \sqrt{2.9^2 + \delta A_{\text{CP}}[\%]^2}, \tag{18}$$

which define the region in the $\kappa, \tilde{\kappa}$ plane allowed by the measured asymmetry. That region is shown in figures 1, 2 by gray dashed lines, with the shaded area corresponding to the region allowed by both measurements, \mathcal{B} and A_{CP} .

The measurement of \hat{R} at the Tevatron by the CDF collaboration sets limits on $(\kappa, \tilde{\kappa})$ through (7). At the 1σ level the allowed region for $(\kappa, \tilde{\kappa})$ is bounded by the inequalities $0.625 < \hat{R} < 1.375$. The lower value turns out to be unattainable, so it does not set any bound. The region delimited by $\hat{R} = 1.375$ is shown in figure 1 by the black solid line. The black dashed lines in that figure show the regions that would be delimited by hypothetical measurements $\hat{R} = 1 \pm 0.1$ and 1 ± 0.05 . We see from the figure that, as expected from the analysis in [7], the bounds set by the Tevatron measurement of \hat{R} are much less constraining than those arising from the asymmetry and branching ratio for $B \rightarrow X_s \gamma$. This is so even in the hypothetical case of an experimental result $\hat{R} = 1 \pm 0.1$ with a 10% measurement error.

Only a 5% measurement uncertainty could yield bounds of the same order of magnitude at most.

We have also performed the same analysis for hypothetical measurements of \hat{R} in pp collisions at the LHC, with the same semileptonic final states and cuts (5), (6). The results are shown in figure 2 (a) for the lower LHC energy and in figure 2 (b) for the higher one. As seen in the figure, the hypothetical experimental results at the LHC would remove significant portions of the region of the $(\kappa, \tilde{\kappa})$ plane allowed by the measurements of the branching ratio and CP asymmetry of $B \rightarrow X_s \gamma$. Whereas this is true already at $\sqrt{s} = 7$ TeV, the constraints set by a measurement of \hat{R} at $\sqrt{s} = 14$ TeV with an experimental uncertainty smaller than, say, 30% would lead to remarkably tighter bounds on $(\kappa, \tilde{\kappa})$ than those currently available. We remark here that the cuts we have applied are rather conservative. Indeed, due to the higher cross sections at LHC collision energies, and to the LHC high luminosity, more stringent cuts could be enforced that could significantly improve the sensitivity of $t\bar{t}\gamma$ production to top dipole moments while still yielding high enough statistics. As a simple illustration of this, we show in figure 3 the bounds that would be obtained at $\sqrt{s} = 14$ TeV if in (5), (6) we substitute the cut $E_T^\gamma > 10$ GeV by $E_T^\gamma > 20$ GeV. As a result of that stricter cut the cross section decreases from $\sigma_{t\bar{t}\gamma}^{\text{SM}} = 0.8034$ pb to 0.4577 pb, which is still almost 25 times larger than the corresponding cross section at the Tevatron. As seen in figure 3, the sensitivity is increased with respect to figure 2 (b) by 30%. Whereas the parton-level analysis carried out here is not the appropriate context to discuss the optimization of experimental cuts, we believe that our results demonstrate the interest of such detailed studies.

On the other hand, the semileptonic channel considered here by analogy with the CDF measurement [5] may not necessarily be the only experimentally relevant one. The question then arises how robust our estimates of the sensitivity to the top dipole moments of $t\bar{t}\gamma$ production are with respect to variations of the selected final state. As a rough attempt to an answer we have considered the process $p\bar{p}$ or $pp \rightarrow t\bar{t} \rightarrow b\bar{b}W^+W^-\gamma$, with only the cut $E_T^\gamma > 10$ GeV, for which we performed the same analysis as described above. In this case we carried out the computations with CALCHEP 3.4 [37]. Besides the expected numerical differences in the results, the conclusions drawn from that alternate analysis are fully consistent with those obtained from the more detailed study presented here.

VI. CONCLUSIONS

We have discussed in the foregoing sections the bounds on the top anomalous dipole moments that can be obtained from measurements of the semi-inclusive decays $B \rightarrow X_s \gamma$, and of $t\bar{t}\gamma$ production at the Tevatron and the LHC. We reviewed the experimental and theoretical determinations of the branching fraction and CP asymmetry of $B \rightarrow X_s \gamma$ and obtained from them bounds on the top MDM and EDM that are significantly more stringent than those reported in the previous literature. The allowed region is defined by the shaded area in the $(\kappa, \tilde{\kappa})$ plane as shown in the figures. Roughly speaking, the MDM term is bounded by $-2 < \kappa < 0.3$ whereas the EDM term is bounded by $-0.5 < \tilde{\kappa} < 1.5$. We can translate these limits in terms of the well known MDM factor $(g-2)/2 = a_t = 3/2 \kappa$: $-3 < a_t < 0.45$ and the EDM factor $d_t = 0.57 \times 10^{-16} \tilde{\kappa}$: $-0.29 < d_t < 0.86 \times 10^{-16} e \text{ cm}$.

We carried out a detailed LO computation of $t\bar{t}\gamma$ production at the Tevatron and the LHC, from which we extracted bounds on the anomalous top MDM and EDM that we compare to those coming from $B \rightarrow X_s \gamma$. From that comparison we conclude that the bounds obtained from the measurement [5] at the Tevatron are too weak to be relevant, but similar studies at the LHC could significantly improve the bounds from $B \rightarrow X_s \gamma$. This conclusion confirms a previous assessment in [7] using a different approach.

The estimates presented in this paper of the direct bounds on the top MDM and EDM that could be obtained from $t\bar{t}\gamma$ production at the LHC, especially at 14 TeV, remove large portions of the parameter space allowed by the indirect bounds from $B \rightarrow X_s \gamma$. Thus, the combination of both sets of bounds could lead to strikingly tighter bounds on $(\kappa, \tilde{\kappa})$ than those coming from $B \rightarrow X_s \gamma$ alone.

Acknowledgments We thank Conacyt and SNI for support.

-
- [1] F. -P. Schilling, Int. J. Mod. Phys. A **27**, 1230016 (2012) [arXiv:1206.4484 [hep-ex]]; W. Bernreuther, J. Phys. G**35**, 083001 (2008); D. Wackeroth, arXiv:0810.4176 [hep-ph]; F. Larios *et al.* Int. J. Mod. Phys. A**21**, 3473 (2006); T. Han, Int. J. Mod. Phys. A **23**, 4107 (2008).
 - [2] K. Kumar, T. M. P. Tait and R. Vega-Morales, JHEP **0905**, 022 (2009).
 - [3] J. F. Kamenik, M. Papucci and A. Weiler, Phys. Rev. D **85**, 071501 (2012)
 - [4] L. Labun and J. Rafelski, arXiv:1209.1046 [hep-ph]; C. Degrande, J. M. Gerard, C. Grojean,

- F. Maltoni and G. Servant, JHEP **1207**, 036 (2012).
- [5] T. Aaltonen *et al.* [CDF Collaboration], Phys. Rev. D **84**, 031104 (2011) [arXiv:1106.3970 [hep-ex]].
- [6] J. Erdmann, arXiv:1206.5696 [hep-ex].
- [7] U. Baur, A. Juste, L. H. Orr and D. Rainwater, Phys. Rev. D **71**, 054013 (2005); Nucl. Phys. Proc. Suppl. **160**, 17 (2006). See also, H. -Y. Zhou, hep-ph/9806323 for a previous study.
- [8] J. L. Hewett and T. G. Rizzo, Phys. Rev. D **49**, 319 (1994).
- [9] W. Bernreuther, R. Bonciani, T. Gehrmann, R. Heinesch, T. Leineweber, P. Mastrolia, E. Remiddi, Phys. Rev. Lett. **95**, 261802 (2005).
- [10] A. Soni and R. M. Xu, Phys. Rev. Lett. **69**, 33 (1992); F. Hoogeveen, Nucl. Phys. B **341**, 322 (1990); M. E. Pospelov and I. B. Khriplovich, Yad. Fiz. **53**, 1030 (1991) [Sov. J. Nucl. Phys. **53**, 638 (1991)].
- [11] T. Ibrahim and P. Nath, Phys. Rev. D **82**, 055001 (2010).
- [12] T. Ibrahim, P. Nath and , Phys. Rev. D **84**, 015003 (2011).
- [13] A. Cordero-Cid, J. M. Hernandez, G. Tavares-Velasco and J. J. Toscano, J. Phys. G **35**, 025004 (2008).
- [14] W. Buchmuller and D. Wyler, Nucl. Phys. B **268**, 621 (1986).
- [15] J. A. Aguilar-Saavedra, M. C. N. Fiolhais, A. Onofre, JHEP **1207**, 180 (2012).
- [16] J. A. Aguilar-Saavedra, Nucl. Phys. B **812**, 181 (2009).
- [17] B. Grzadkowski, Z. Hioki, K. Ohkuma, J. Wudka, Nucl. Phys. B **689**, 108 (2004).
- [18] B. Grzadkowski, M. Iskrzynski, M. Misiak, J. Rosiek, JHEP **1010**, 085 (2010).
- [19] G. Aad *et al.* [ATLAS Collaboration], JHEP **1206**, 088 (2012).
- [20] C. Zhang, N. Greiner, S. Willenbrock, Phys. Rev. D **86**, 014024 (2012).
- [21] U. Baur, M. Buice and L. H. Orr, Phys. Rev. D **64**, 094019 (2001).
- [22] J. Alwall, M. Herquet, F. Maltoni, O. Mattelaer, T. Stelzer, J. High Energy Phys. **06**, 128 (2011)
- [23] N. D. Christensen, C. Duhr, Comput. Phys. Commun. **180**, 1614 (2009).
- [24] S. Ask *et al.*, arXiv:1209.0297.
- [25] A. J. Buras, M. Misiak, M. Munz and S. Pokorski, Nucl. Phys. B **424**, 374 (1994); A. L. Kagan and M. Neubert, Eur. Phys. J. C **7**, 5 (1999).
- [26] W. Altmannshofer, P. Paradisi and D. M. Straub, JHEP **1204**, 008 (2012).

- [27] E. Lunghi and J. Matias, JHEP **0704**, 058 (2007).
- [28] T. Becher and M. Neubert, Phys. Rev. Lett. **98**, 022003 (2007).
- [29] M. Misiak, H. M. Asatrian, K. Bieri, M. Czakon, A. Czarnecki, T. Ewerth, A. Ferroglia and P. Gambino *et al.*, Phys. Rev. Lett. **98**, 022002 (2007).
- [30] J. R. Andersen and E. Gardi, JHEP **0701**, 029 (2007).
- [31] G. Paz, arXiv:1011.4953 [hep-ph].
- [32] The Heavy Flavor Averaging Group, <http://www.slac.stanford.edu/xorg/hfag>.
- [33] T. Hurth and F. Mahmoudi, arXiv:1211.6453 [hep-ph].
- [34] A. L. Kagan and M. Neubert, Phys. Rev. D **58**, 094012 (1998)
- [35] M. Benzke, S. J. Lee, M. Neubert and G. Paz, Phys. Rev. Lett. **106**, 141801 (2011).
- [36] Gil Paz, arXiv:1212.4546 [hep-ph].
- [37] A. Belyaev, N. Christensen, A. Pukhov, arXiv:1207.6082; A.Pukhov, hep-ph/0412191; A.Pukhov et al, Preprint INP MSU 98-41/542, arXiv:hep-ph/9908288.

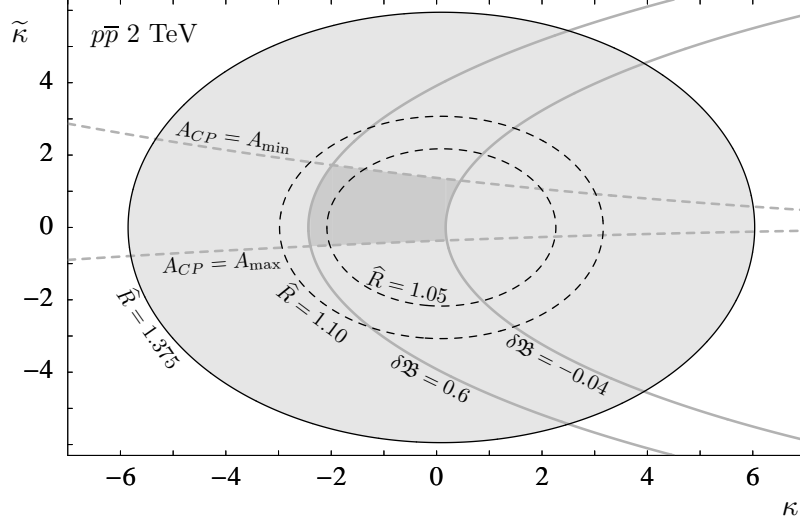


FIG. 1: The allowed parameter space for the anomalous magnetic and electric dipole moments of the top quark. Gray solid lines: region allowed by the experimental results for the branching ratio for $B \rightarrow X_s \gamma$, see eq. (11). Gray dashed lines: region allowed by the experimental results for the CP asymmetry for $B \rightarrow X_s \gamma$, see eq. (18). Black solid line: region allowed by the CDF measurement of \hat{R} for $t\bar{t}\gamma$ production at $\sqrt{s} = 2$ TeV, see eq. (7), with the cuts (5), (6). Black dashed lines: regions allowed by the values of \hat{R} indicated in the figure.

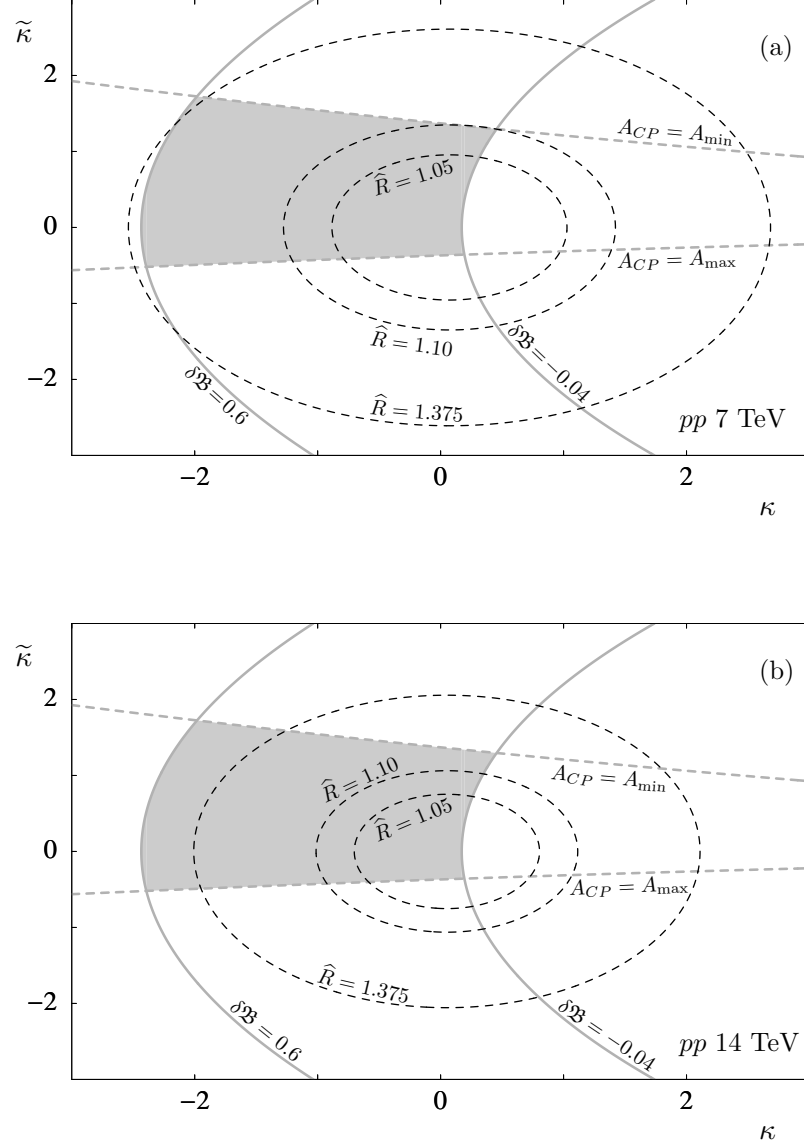


FIG. 2: Gray lines as in previous figure. Black solid and dashed lines delimit the regions allowed by hypothetical measurements of \hat{R} for $t\bar{t}\gamma$ production with the cuts (5), (6) at the LHC at (a) $\sqrt{s} = 7$ TeV, (b) $\sqrt{s} = 14$ TeV.

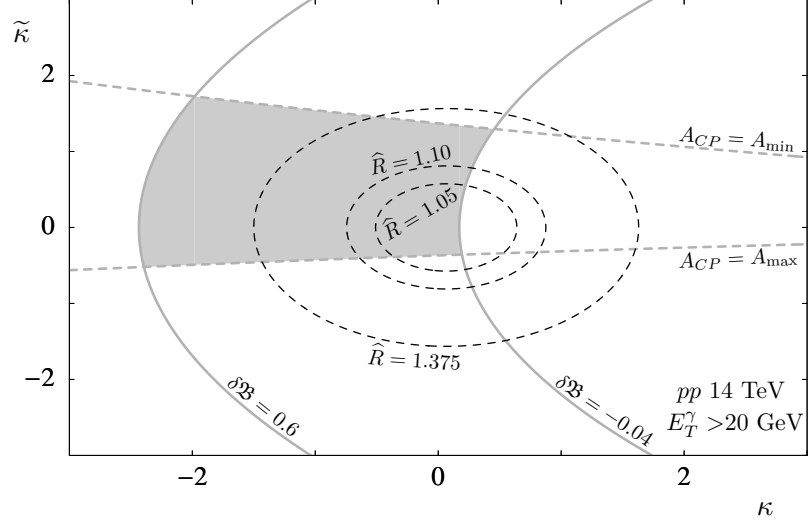


FIG. 3: Same as figure 2(b), but with the stricter cut $E_T^\gamma > 20$ GeV.